Controlling nucleation and growth of water using hybrid hydrophobic-hydrophilic surfaces

CONTROLLING NUCLEATION AND GROWTH OF WATER USING HYBRID HYDROPHOBIC-HYDROPHILIC SURFACES

Kripa K. Varanasi[1, a], Tao Deng[2]
[1]Department of Mechanical Engineering
Massachusetts Institute of Technology, Cambridge, MA
[2] GE Global Research Center, Niskayuna, NY

ABSTRACT

Heterogeneous nucleation of water plays an important role in wide range of natural and industrial processes. Though heterogeneous nucleation of water is ubiquitous and everyday experience, spatial control of this important phenomenon is extremely difficult. Here we show, for the first time, that spatial control in the heterogeneous nucleation of water can be achieved by manipulating the local nucleation energy barrier and nucleation rate via the modification of the local intrinsic wettability of a surface by patterning hybrid hydrophobic-hydrophilic regions on a surface. Such ability to control water nucleation could address the condensation-related limitations of superhydrophobic surfaces, and has implications for efficiency enhancements in energy and desalination systems.

KEY WORDS: nucleation, condensation, hydrophobic, hydrophilic, wetting, superhydrophobic

NOMENCLATURE

ΔG free energy barrier, J
r^* critical nucleation radius, m
J nucleation rate, m
k Boltzmann constant
T temperature, K
p pressure, Pa

Greek symbols

σ surface energy (N/m)
θ theta

Subscripts

lv liquid-vapor

INTRODUCTION

Heterogeneous vapor-to-liquid nucleation of water is an everyday phenomenon and plays an important role in the formation of rain drops [1], dew [2], and in several engineering applications such as condensation heat transfer [3], steam nucleation in power turbines [4], detection of aerosols in atmosphere [5], recovery of atmospheric water [6], distillation, desalination, etc. Classical nucleation theory [7,8] predicts that an energy barrier that depends strongly on the intrinsic wettability of the surface has to be overcome for the formation of initial liquid nuclei on the surface [8-12]. Since the intrinsic wettability of regular surfaces is spatially uniform, heterogeneous nucleation of water droplets occurs in a random fashion without any particular spatial preference. This effect accounts for the recent observations on the loss of superhydrophobic properties of lotus leaves [13] and associated synthetic surfaces under condensation [14,15,16] and has been identified as a critical limitation of superhydrophobic surfaces [17]. By taking advantage of the strong dependence of the nucleation energy barrier and nucleation rate on wettability, we report here for the first time that heterogeneous nucleation can be spatially controlled by the manipulation of the local intrinsic wettability of a surface. Using an environmental scanning electron microscope (ESEM), we show that water droplets preferentially nucleate on the hydrophilic regions of hybrid hydrophobic-hydrophilic surfaces we fabricated. This ability to control nucleation-level phenomena could more broadly lead to efficient condensers in power generation and desalination, reduce moisture-induced efficiency losses in steam turbines, and high-performance heat pipes for electronics cooling applications.

NUCLEATION: BACKGROUND AND LIMITATIONS OF SUPERHYDROPHOBIC SURFACES

Condensation of water vapor from moist air and steam has been an active area of research for more than a century [18]. According to Volmer's classical nucleation theory [7,8] the free energy barrier ΔG for the formation of a liquid nucleus on a flat surface depends strongly on the intrinsic wettability of the surface via the contact angle θ:

$$\Delta G = \frac{\pi \sigma_{lv} r^{*2}}{3}(2 - 3\cos\theta + \cos^3\theta) \quad (1)$$

where σ_{lv} is the liquid-vapor surface energy and r^* is the critical radius. The formula for the critical radius is given by Kelvin's classical equation [19]: $\ln(p/p_\infty) = 2\sigma_{lv}/n_l kTr^*$, where p is the vapor pressure over a curved interface of radius r^* and p_∞ is the equilibrium vapor pressure above a flat surface of the condensed phase at temperature T, n_l is the number of molecules per unit volume of the liquid, and k is the Boltzmann constant. The intrinsic wettability of the surface has a strong effect on the nucleation rate J, via the inverse exponential dependence on ΔG:

$$J = J_o \exp(-\Delta G/kT) = J_o \exp(\pi \sigma_{lv} r^{*2}(2 - 3\cos\theta + \cos^3\theta)/3kT) \quad (2)$$

where J_o is a kinetic constant. Therefore, a surface with spatially uniform intrinsic wettability will be characterized by a spatially uniform ΔG and J, and as a result heterogeneous nucleation on such surfaces occurs without any particular spatial preference as a random process. This phenomenon was

[a] Corresponding Authors: Prof. Kripa K. Varanasi (varanasi@mit.edu), Dr. Tao Deng (dengt@research.ge.com)

978-1-4244-5343-6/10/$26.00 ©2010 IEEE

evident in our ESEM study of water vapor condensation on a superhydrophobic surface comprising of an array of hydrophobic silicon posts as shown in Fig. 1. Because of the spatially uniform intrinsic wettability of the surface (see methods in Appendix), ΔG and J are also spatially uniform resulting in droplet nucleation all over the post surfaces (post tops, side walls, and valleys). This non-preferential nucleation results in the formation of a mixture of Cassie-[20] and Wenzel-type[21] droplets under condensation in contrast to the usually observed Cassie behavior in the case of sessile [22,23] and bouncing droplets [24] on such surfaces. This nucleation-driven phenomenon results in the loss of the metastable non-wetting states on textured hydrophobic surfaces and accounts for the observed loss of superhydrophobic properties of lotus leaves and lotus-inspired surfaces and renders them ineffective under condensation [13-17]

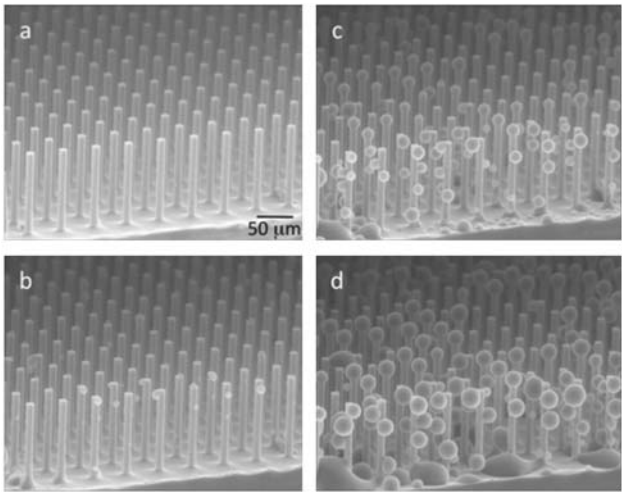

Fig. 1. ESEM images of the condensation of water vapor on a superhydrophobic surface comprising of an array of hydrophobic square posts with width, edge-to-edge spacing, and aspect ratio of 15∝m, 30∝m, 7, respectively. (**a**) Dry surface. (**b** to **d**) Snapshot images of the condensation phenomenon on the surface. The intrinsic contact angle of the hydrophobic coating on the posts is ~110^o and the effective contact angle of the surface measured via sessile droplet technique with a 1∝L drop is ~155^o. The surface is maintained at a temperature of 274K by means of a cold stage accessory of the ESEM. At the beginning of the experiment the chamber pressure is maintained ~ 400 Pa, well below the saturation pressure to ensure a dry surface. The vapor pressure in the chamber is then slowly increased until droplet nucleation is observed. Droplet nucleation occurs without any particular spatial preference due to the uniform intrinsic wettability of the surface. These droplets grow, coalesce and would ultimately result in a mixture of Cassie and Wenzel type droplets [30].

CONTROLLING NUCLEATION USING HYBRID HYDROPHOBIC-HYDROPHILIC SURFACES

From the above discussion, the question that naturally arises is: can one achieve spatial control in the heterogeneous nucleation of water? If this spatial control were possible, droplets can be made to preferentially nucleate on post tops, thereby forcing Cassie-type behavior on textured surfaces even under condensation. Such an approach can result in superior droplet shedding surfaces even in condensation environments and lead to high-quality dropwise condensation, since Cassie droplets have lower hysteresis. One possible approach to answer this question lies in the dependence of the nucleation energy barrier and rate on contact angle as given by Eqs. 1-2. As shown in Fig. 2, the nucleation energy barrier continuously increases with contact angle indicating that hydrophobic surfaces have higher nucleation energy barrier when compared to hydrophilic surfaces, under identical conditions. For example, the nucleation energy barrier for a hydrophobic surface with a contact angle of 110^o would be about 117 times higher than that of a hydrophilic surface with a contact angle of 25^o. Consequently, the nucleation rate on the hydrophilic surface would be significantly higher than that on the hydrophobic surface due to the inverse exponential dependence of the nucleation rate on the energy barrier. An estimate of the nucleation rate for a typical saturation ratio p/p_∞ (corresponding to a critical radius of about ~ 2nm at temperature T= 274K) indicates that the nucleation rate on the hydrophilic surface with a contact angle of 25^o is zillions of orders of magnitude higher than that on the hydrophobic surface with a contact angle of 110^o (by a factor of $\sim 10^{129}$). Hence, a surface patterned with hydrophobic and hydrophilic regions that have significant difference in intrinsic wettability can be potentially used to create spatial preference for nucleation, where nucleation would be favoured on the hydrophilic regions of the surface. The larger the difference between the intrinsic wettability of these regions, the stronger is the propensity to cause this preference [30].

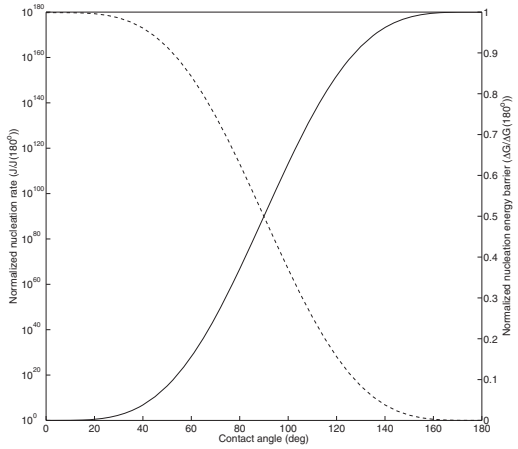

Fig. 2. Normalized nucleation energy barrier (ΔG normalized by $\Delta G(180^o) = 4\pi\sigma_{lv} r^{*2}/3)$) (solid line) and normalized nucleation rate (J normalized by $J(180^o) = J_o \exp(-4\pi\sigma_{lv} r^{*2}/3kT)$) (dashed line) for heterogeneous nucleation of water on a plane surface as a function of the contact angle. The normalized nucleation rate is plotted for a typical saturation ratio $p/p_\infty = 1.7$. The plot indicates that the energy barrier continuously increases with

contact angle and is high for hydrophobic surfaces and low for hydrophilic surfaces. Consequently, the nucleation rate on a hydrophilic surface with contact angle of 25° is zillions of orders of magnitude higher than that on a hydrophobic surface with contact angle of 110°. The nucleation energy barrier seems to approach zero for $\theta = 0°$, however, at very low contact angles the energy of the contact line has to be taken into consideration.

To verify this concept, we fabricated two types of hybrid hydrophobic-hydrophilic surfaces (see methods section in Appendix) and conducted condensation experiments in an ESEM. The first surface consists of alternating hydrophobic and hydrophilic segments on a silicon wafer with intrinsic contact angles of ~110° and ~25° degrees, respectively. The hydrophilic regions are made up of the native oxide on the Si wafer, while the hydrophobic regions are modified with fluorosilane. These segments are 25 microns in width and were fabricated via micro-contact printing using a prefabricated polydimethylsiloxane (PDMS) stamp (see methods section in Appendix). Condensation experiments were conducted on these surfaces in the ESEM and the corresponding images (taken over a span of 30s) are shown in Fig. 3. These ESEM images clearly demonstrate that large difference in the intrinsic wettability of the hydrophilic and hydrophobic segments results in preferential nucleation and subsequent droplet growth on the hydrophilic segments of the hybrid surface.

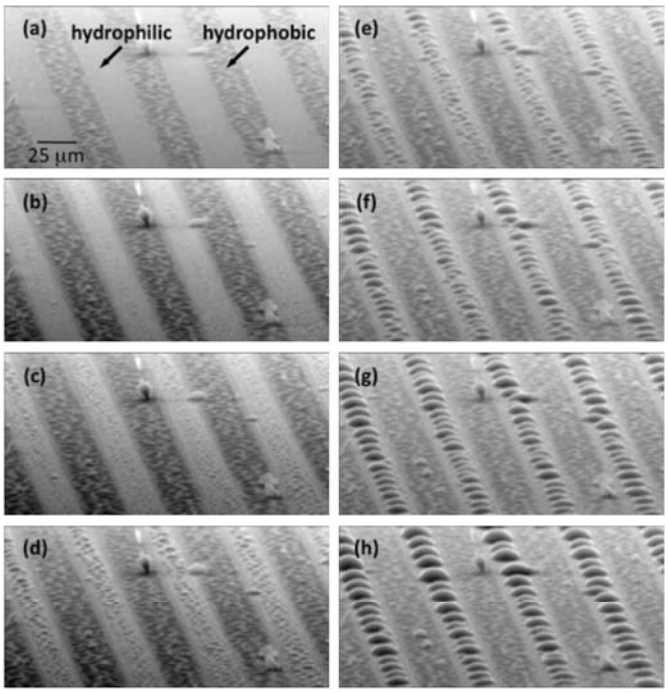

Fig. 4. ESEM images of condensation of water vapor on a surface with alternating hydrophobic and hydrophilic segments. (**a**) Dry surface. (**b** to **h**) Snapshot images of the condensation phenomenon on the surface. The width of the segments is about 25∝m. The intrinsic contact angle of the hydrophilic regions is ~25° and that of the hydrophobic regions is ~110°. The surface was maintained at a temperature of 274K by means of a cold stage accessory of the ESEM. At the beginning of the experiment the chamber pressure is maintained ~ 400 Pa, well below the saturation pressure to ensure a dry surface. The vapor pressure in the chamber is then slowly increased until droplet nucleation is observed. Droplets are observed to preferentially nucleate and grow on the hydrophilic regions due to the lower ΔG and significantly higher J.

The second surface is a textured surface consisting of an array of hydrophobic posts with hydrophilic tops. As in the case of the hybrid segments the intrinsic contact angle of the hydrophobic regions is ~110° and that of the hydrophilic regions is ~25°. This surface was fabricated via lithography combined with UV-assisted surface modification approach that is described in the methods section in Appendix. The hydrophilic tops are made up of deposited silicon dioxide while the hydrophobic sidewalls and valleys are modified with fluorinated hydrocarbon molecules. The fabrication results were validated by two independent techniques: Time of Flight-Secondary Ion Mass Spectroscopy (ToF-SIMS) and Auger analysis. As shown in Fig. 4, ToF-SIMS analysis of the surface revealed that the post sidewalls and valleys were indeed modified to fluorine-rich surfaces while the post tops remain rich in oxygen. The results from Auger analysis were consistent with the ToF-SIMS results and showed that the post tops were rich in oxygen whereas the sidewalls and the valleys were rich in fluorine. Next, we conducted simultaneous ESEM experiments on such a hybrid surface and a superhydrophobic surface with identical texture. The images from these experiments are shown in Fig. 6. These ESEM images clearly demonstrate that nucleation and subsequent growth of droplets occur preferentially on the hydrophilic post tops of the hybrid surface when compared to the random nucleation of droplets on the identically textured superhydrophobic surface with uniform wettability (drops grow in the valleys, tops, and sides of the posts).

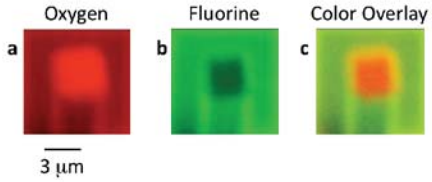

Fig. 5. ToF-SIMS analysis of the hydrophobic post with hydrophilic top. (a) Oxygen map. (b) Fluorine map. (c) Color overlay showing the tops are rich in oxygen whereas sidewalls and the valleys are rich in fluorine.

The textured hybrid surface discussed above is reminiscent of the water-capturing surface of the Namib beetle [25,26]. Our results complement the findings of Parker and Lawrence [25] and Zhai et.al. [26], who suggest that the Namib beetle captures water by collecting small airborne water droplets (1-40 ∝m diameter) present in the early morning fog on the hydrophilic regions of its surface. In addition to this mechanism of trapping airborne droplets, we propose that the beetle's surface can capture water by *direct and preferential heterogeneous vapor-to-liquid nucleation*

onto the hydrophilic regions on the surface. Subsequently, these droplets grow by further condensation and coalescence and roll into the beetle's mouth. Thus, we believe that the beetle's surface is nature's version of dropwise condensing surface.

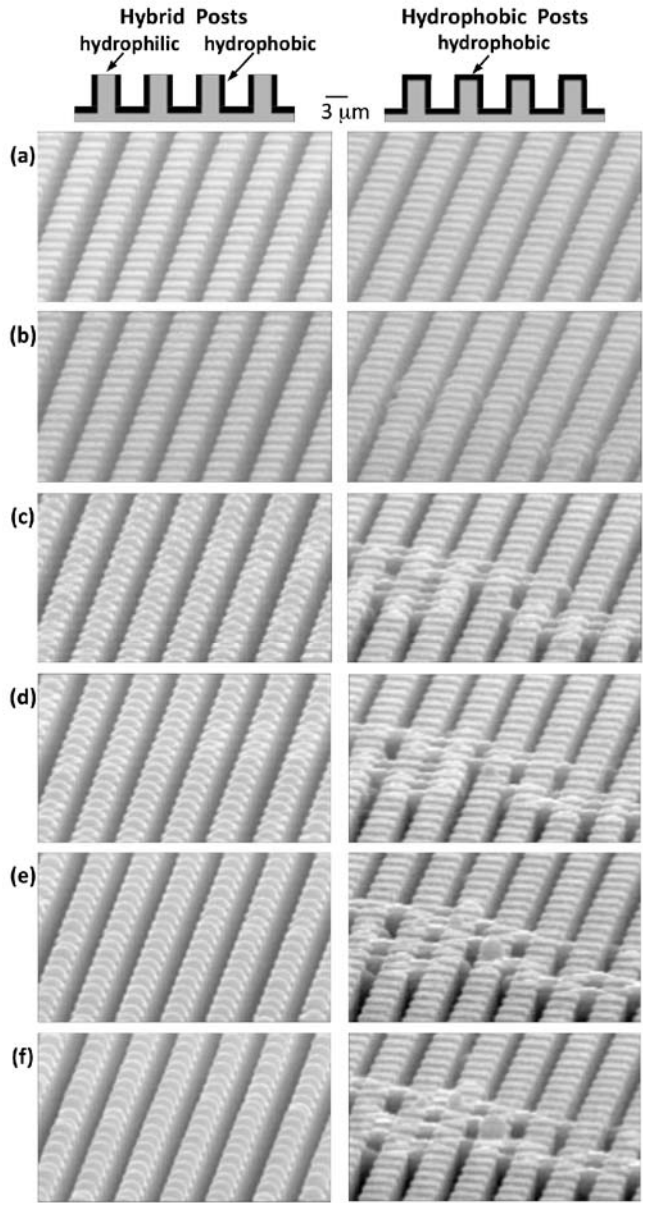

Fig. 5. Comparison of the condensation behavior on a hybrid surface consisting of hydrophobic posts with hydrophilic tops (left) with that of a superhydrophobic surface consisting of hydrophobic posts (right). (**a**) Dry surface. (**b** to **f**) Snapshot images of the condensation phenomenon on the surfaces. The geometry of the posts is identical for both surfaces with width, edge-to-edge spacing, and aspect ratio of 3∝m, 1.5∝m, and 3, respectively. The intrinsic contact angle of the hydrophilic regions is ~25^{o} and that of the hydrophobic regions is ~110^{o}. The surfaces were maintained at a temperature of 274 K by means of a cold stage accessory of the ESEM. At the beginning of the experiment the chamber pressure is maintained ~ 400 Pa, well below the saturation pressure to ensure a dry surface. The vapor pressure in the chamber is then slowly increased until droplet nucleation is observed. Droplets are observed to preferentially nucleate and grow on the hydrophilic post tops for the hybrid surface (left) whereas droplets nucleate and grow everywhere without any spatial preference on the superhydrophobic surface (right).

CONCLUSIONS

In summary, we demonstrate that spatial control in the heterogeneous nucleation of water can be achieved. Manipulation of the local wettability of a surface by patterning it with hydrophobic and hydrophilic regions (that have significant difference in their intrinsic wettability) will result in preferential nucleation on the hydrophilic regions. These studies provide a pathway to better understand the fundamentals of heterogeneous nucleation of water, and other areas such as ice formation and crystal nucleation [27]. In contrast to the random nucleation behavior of superhydrophobic surfaces, textured hydrophobic surfaces with hydrophilic tops promote nucleation and growth of Cassie-type droplets and can therefore exhibit superior droplet shedding properties under condensation. As a result, these hybrid surfaces have a great potential to enhance condensation heat transfer [28] and could broadly lead to efficient condensers in power generation and desalination, reduce moisture-induced efficiency losses in steam turbines, and high-performance heat pipes for electronics cooling applications [29].

Appendix

A. Materials and Methods

A.1 Surface with hydrophobic silicon posts: The silicon posts used in the experiments were fabricated using standard photolithography process. A photomask with square windows was used during photolithography and the patterns were transferred into the photoresist. Next, reactive ion etching (RIE) in an inductively coupled plasma process was used to transfer the pattern into silicon with high aspect ratio. A thin coating of (tridecafluoro –1,1,2,2 –tetrahydrooctyl) trichlorosilane (Gelest, Inc., Morrisville, PA) was then deposited onto the silicon surface through vapor-phase deposition to generate hydrophobic posts.

A.2 Surface with alternate hydrophobic-hydrophilic segments: The silicon surface with hydrophobic-hydrophilic segments was fabricated via micro-contact printing.[2] A polydimethysiloxane (PDMS) mold was fabricated via replication process against a silicon master with line patterns. The replication process involved degassing and pouring the PDMS precursor, Sylgard 184 (Dow Corning, Midland, MI) on top of the silicon master surface, further degassing for 30 minutes, curing in an oven at 60^{0} C for 2 hours, and peeling the replicated mold off from the silicon master. The PDMS mold was then coated with a thin layer of (tridecafluoro –1,1,2,2 –tetrahydrooctyl) trichlorosilane through vapor phase

deposition. The coated PDMS mold was brought into contact with a pre-cleaned silicon substrate for ~1min. After the release of the mold from silicon, the strip patterns of fluorosilane were transferred onto the silicon surface.

A.3 Surface with post array comprising of hydrophilic tops and hydrophobic sidewalls and valleys: Silicon wafers coated with a thick oxide layer (~ 300nm) were used as the starting material. Post structures were fabricated on these wafers using standard photolithography process. This process resulted in posts that had a thick oxide layer on the tops but only a thin native-oxide layer on the post sidewalls and valleys. Next, these post structures were immersed in a 6:1 mixture of NH_4F (40wt% aqueous) and HF (48 wt% aqueous) for about a minute to remove the native-oxide layer on the sidewalls and valleys. The thicker oxide layer on the post tops was unaffected and remained intact during this etching process. These etched samples were then covered with a thin layer of 1H,1H,2H-perfluoro-1-dodecene (Aldrich) in a nitrogen-purged Teflon cell. Next, illumination with UV radiation (254nm) for 2 hours through the quartz window of the cell grafted the fluorinated dodecene onto the exposed silicon surfaces of the post sidewalls and valleys and rendered them hydrophobic.[3] The fabrication results were validated by two independent techniques: Time of Flight-Secondary Ion Mass Spectroscopy (ToF-SIMS) and Auger analysis. As shown in Fig. 4, ToF-SIMS analysis of the surface revealed that the post sidewalls and valleys were indeed modified to fluorine-rich surfaces while the post tops remain rich in oxygen.

References

[1] N. H. Fletcher, N. H. *The Physics of Rain Clouds* (Cambridge University Press, Cambridge, 1962).
[2] R. Eiden, J. Burkhardt, O. Burkhardt, *J. Aerosol Sci*. **25**, 367 (1994).
[3] W. M. Rohsenow, J. P. Hartnett, Y. I. Cho, *Handbook of Heat Transfer* (McGraw-Hill, New York, 1998).
[4] K. C. Cotton, *Evaluating and Improving Steam Turbine Performance* (Cotton Fact Inc. Publishers, 1998).
[5] H. R. Pruppacher, J. D. Klett *Microphysics of Clouds and Precipitation* (Kluwer Academic Publishers, 1997).
[6] A. R. Jumikis, *Soil Sci.* **100**, 83 (1965).
[7] M. Volmer, A. Weber, *Z. Phys. Chem.* (Germany) **119**, 277-301 (1925).
[8] R. A. Sigsbee, *Nucleation* (A. C. Zettlemoyer ed, Marcel Dekker, New York, 1969).
[9] J. A. Koutsky, A. G. Walton, E. Baer, *Surf. Sci.* **3**, 165 (1965).
[10] P. C. Mahata, D. J. Alofs, *J. Atmos. Sci.* **32**, 116 (1975).
[11] D. Beysens, C. M. Knobler, *Phys. Rev. Lett.* **57**, 1433 (1986).
[12] H. Zhao, D. Beysens, *Langmuir* **11**, 627 (1995).
[13] Y. T. Cheng, D. E. Rodak, *Appl. Phys. Lett*. **86**, 144101 (2005).
[14] R. D. Narhe, D. A. Beysens, Phys. Rev. Lett. **93**, 076103-1 (2004); Langmuir **23**, 6486 (2007).
[15] Y. Zheng, D. Han, J. Zhai and L. Jiang, Appl. Phys. Lett., **92**, 084106, (2008).
[16] C. C. Yung and B. Bushan, J. Microsc., **229**, 127 (2008).
[17] C. Dorrer and J. Ruhe, Soft Matter, **5**, 51, (2009)
[18] C. T. R. Wilson, Phil. Trans. R. Soc. Lond. A **189**, 265 (1897).
[19] Lord Kelvin, Proc. Roy. Soc. Edinb. **7**, 63 (1870).
[20] A. B. D. Cassie, S. Baxter, Trans. Faraday Soc. **40**, 546 (1944).
[21] R. N. Wenzel, Ind. Eng. Chem. **28**, 988 (1936).
[22] A. Lafuma, D. Quere, Nat. Mater. **2**, 457 (2003).
[23] N. A. Patankar, Langmuir, **24**, 6262 (2008).
[24] T. Deng, K. K. Varanasi, M. Hsu, N. Bhate, C. Keimel, J. Stein, M. Blohm, Appl. Phys. Lett. **94**, 133109 (2009).
[25] A. R. Parker, C. R. Lawrence, *Nature* **414**, 33 (2001).
[26] L. Zhai, et.al., *Nano Lett.* **6**, 1213 (2006).
[27] J. Aizenberg, A. J. Black, G. M. Whitesides, Nature **398**, 495 (1999).
[28] K.K. Varanasi et.al., US Patent Application 20070028588, (2005).
[29] K.K. Varanasi and T. Deng, US Patent Application 12/254561 (2008).
[30] K. K. Varanasi, M. Hsu, N. Bhate, W. Yang, T. Deng, 95, Applied Physics Letters, 094101 (2009).